Thermochemical Studies of *N*-Methylpyrazole and *N*-Methylimidazole

Stephanie M. Villano, Adam J. Gianola, Nicole Eyet, Takatoshi Ichino, Shuji Kato, Veronica M. Bierbaum,* and W. Carl Lineberger*

JILA, University of Colorado and the National Institute of Standards and Technology, and Department of Chemistry and Biochemistry, University of Colorado, Boulder, Colorado 80309-0440

Received: May 7, 2007; In Final Form: June 18, 2007

The 351.1 nm photoelectron spectra of the *N*-methyl-5-pyrazolide anion and the *N*-methyl-5-imidazolide anion are reported. The photoelectron spectra of both isomers display extended vibrational progressions in the $\tilde{X}^2A'$ ground states of the corresponding radicals that are well reproduced by Franck−Condon simulations, based on the results of B3LYP/6-311++G(d,p) calculations. The electron affinities of the *N*-methyl-5-pyrazolyl radical and the *N*-methyl-5-imidazolyl radical are 2.054 ± 0.006 eV and 1.987 ± 0.008 eV, respectively. Broad vibronic features of the $\tilde{A}^2A''$ states are also observed in the spectra. The gas-phase acidities of *N*-methylpyrazole and *N*-methylimidazole are determined from measurements of proton-transfer rate constants using a flowing afterglow-selected ion flow tube instrument. The acidity of *N*-methylpyrazole is measured to be $\Delta_{acid}G_{298}$ = 376.9 ± 0.7 kcal mol^{-1} and $\Delta_{acid}H_{298}$ = 384.0 ± 0.7 kcal mol^{-1}, whereas the acidity of *N*-methylimidazole is determined to be $\Delta_{acid}G_{298}$ = 380.2 ± 1.0 kcal mol^{-1} and $\Delta_{acid}H_{298}$ = 388.1 ± 1.0 kcal mol^{-1}. The gas-phase acidities are combined with the electron affinities in a negative ion thermochemical cycle to determine the C5−H bond dissociation energies, D_0(C5−H, *N*-methylpyrazole) = 116.4 ± 0.7 kcal mol^{-1} and D_0(C5−H, *N*-methylimidazole) = 119.0 ± 1.0 kcal mol^{-1}. The bond strengths reported here are consistent with previously reported bond strengths of pyrazole and imidazole; however, the error bars are significantly reduced.

Introduction

Azoles are nitrogen-containing five-membered ring heteroaromatic compounds whose structures are analogous to cyclopentadiene, C_5H_6, where a N atom has replaced one or more C−H groups. These compounds constitute an important class of heterocycles whose structures appear as fundamental units in biomolecules,[1] pharmaceuticals,[2,3] ionic liquids,[4,5] dyes,[6,7] explosives,[8] and fuels.[9−11] Sound knowledge of the thermochemistry, especially the bond dissociation energies (BDEs), of these compounds is important to fields such as combustion chemistry[12] and transition metal coordination chemistry.[13−16]

The vast majority of information in the literature about azoles has focused on pyrrole, C_4NH_5. It is postulated that the thermal decomposition of pyrrole, along with other N-heterocycles that are contained in coal, leads to the formation of NO_x species in the atmosphere.[17,18] The thermal decomposition of pyrrole has been investigated by two groups using shock tube pyrolysis.[19,20] The initial decomposition step proceeds by a hydrogen-atom transfer from the nitrogen to the adjacent carbon (C2 carbon) to form pyrrolenine, followed by the cleavage of the C2−N bond to produce a ring-opened structure.[19,21] This acyclic structure further decomposes by C−C bond cleavage. In contrast, there is evidence that thermal decomposition of pyridine, the six-membered heterocycle that contains one nitrogen atom, is initiated by the cleavage of the C2−H bond.[22] The difference between these two initiation steps, in part, may be attributed to the difference in C−H bond strengths of the five- and six-membered heterocycles. The C2−H and N−H bond strengths of pyrrole were measured by Blank et al.[23] using photofragment translational spectroscopy to be 112.5 ± 1 and 88 ± 2 kcal mol^{-1}, respectively. Later experiments,[24,25] however, have not observed a C−H bond dissociation process in the photochemistry of pyrrole and find the N−H BDE to be higher, 93.92 ± 0.11 kcal mol^{-1}. In contrast, the corresponding C2−H BDE of pyridine is reported to be much lower at 105 kcal mol^{-1}; for the C−H bonds that do not have an adjacent nitrogen atom (C3 and C4 carbons), the BDEs increase to 112 kcal mol^{-1}.[26] In contrast to this extensive knowledge of these mononitrogen heterocycles, much less is known about the nitrogen heterocycles that contain additional nitrogen atoms in the ring.

Our research program has utilized negative ion spectroscopy along with gas-phase ion chemistry to study several azoles.[27−31] Negative ion spectroscopy provides thermodynamic information such as electron affinities and term energies, allows for the measurement of vibrational frequencies, and gives insight into the molecular structure of both the anion and radical species.[32] Gas-phase ion chemistry studies include the measurement of the forward and reverse proton-transfer reaction rate constants in order to determine the gas-phase acidity relative to a reference acid. These techniques are complementary since the electron affinity (EA) of the neutral radical can be combined with the gas-phase acidity ($\Delta_{acid}G_{298}$) to determine the BDE using a negative ion thermochemical cycle.[33,34]

Using these techniques we have previously investigated the thermodynamic properties of pyrazole (I) and imidazole (II).[27,29,30] In that work, the 1-azolide anion was formed by deprotonation of the azole by hydroxide at the most acidic site, the N−H bond. Photoelectron spectra of the 1-azolide anions were reported along with a discussion of the electronic structure of the corresponding radical. The gas-phase acidity of the N−H bond was measured using proton-transfer equilibrium measurements and the N−H BDE was obtained. In addition to deprotonation at the nitrogen, deprotonation also occurred at the next acidic site, the carbon adjacent to the N−H group (C5 carbon),

10.1021/jp073475m CCC: $37.00
Published on Web 08/16/2007

allowing for the assignment of the EA of the C5 radical. In both the pyrazolide and the imidazolide anion spectra, C5 deprotonation was only observed when the azolide anion was prepared by proton transfer to hydroxide. When the azole anion was prepared by proton transfer to O^-, only the 1-azolide anion spectra were seen. The acidity ($\Delta_{acid}G_{298}$) of the C5−H bond was bracketed between that of water and the hydroxy radical at 380 ± 4 kcal mol^{-1}. The C5−H BDE was then determined to be 121 ± 4 kcal mol^{-1} for pyrazole and 119 ± 4 kcal mol^{-1} for imidazole. The large error bars reflect the acidity gap between water and hydroxy radical. However, even when suitable reference acids are available, quantitative determination of the gas-phase acidities and C−H BDEs is difficult when there are multiple acidic sites in the molecule.

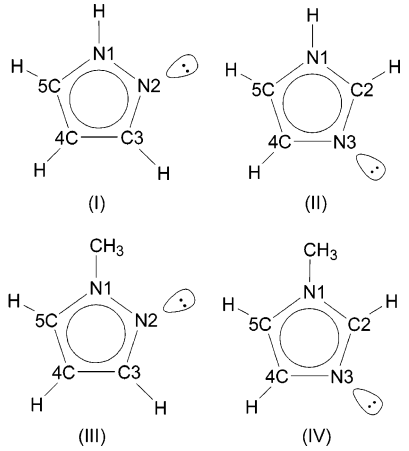

Measurements of gas-phase proton-transfer reactions generally determine the gas-phase acidity (and hence the BDE) of only the most acidic site of a hydrocarbon. This limitation, in part, is due to the inherent difficulty in preparing the more basic anion from neutral precursors. One commonly used method to probe the acidity of the less acidic site is fluorodesilylation of substituted trimethylsilanes.[35−40] This method allows for the preparation of regiospecific carbanions whose acidity can then be bracketed between two reference acids.

A second technique that allows for acidity measurements on molecules with multiple acidic sites uses a dual-cell Fourier transform mass spectrometer.[41,42] In this method a mixture of isomeric anions is formed in the source region. To prevent catalyzed isomerization of the more basic anion to the less basic species, the ion mixture is extracted into a second chamber, which is free of neutral precursors. With the use of this technique a lower bound acidity can be found for the less acidic proton. This method has recently been applied to determine the acidities of the N1 and N3 sites of uracil[41] and the N9 and N10 sites of adenine and adenine derivatives.[42] This technique, however, requires a sufficient difference in the acidity of the two sites so that bracketing experiments can be used; moreover, the time scale for ion extraction must be shorter than for ion isomerization.

The principal motivation of this work is to improve the precision of the C5−H BDE of pyrazole and imidazole through the investigation of the corresponding *N*-methylated species (III and IV). *N*-Methylation of pyrazole and imidazole blocks the nitrogen site and makes the C5 position the most acidic site, without significantly changing the C−H bond energetics (as discussed below). Here we report the photoelectron spectra of *N*-methylpyrazolide anion and *N*-methylimidazolide anion, as well as electronic structure calculations, which aid in the interpretation and assignment of the spectra. The gas-phase acidities of the C5 positions in *N*-methylpyrazole and *N*-methylimidazole were measured, and these measurements are used to determine the C5−H BDE.

Experimental Methods

Negative Ion Photoelectron Spectroscopy. The ultraviolet negative ion photoelectron spectra of the *N*-methylpyrazolide anion and the *N*-methylimidazolide anion were obtained with a flowing afterglow-negative ion photoelectron spectrometer that has been described in detail previously.[32,43,44] The *N*-methylpyrazolide and *N*-methylimidazolide anions are prepared by proton abstraction from *N*-methylpyrazole and *N*-methylimidazole, respectively, using hydroxide (OH^-) as a base, downstream of a microwave discharge source. As will be shown below, deprotonation occurs on the C5 carbon. Ions are thermalized to ∼298 K by collisions with He buffer gas (∼0.5 torr, 3−10 ms residence time).[43] The ions can be further cooled by surrounding the source flow tube with a liquid nitrogen jacket. Prior experience with this technique suggests that the resulting ions are prepared in the ∼200 K range.[45] Negative ions, extracted from the flowing afterglow source region, are accelerated to 735 eV and focused for mass selection by a Wien filter. The mass-selected ion beam is refocused and decelerated to 35 eV and crossed with a 351.1 nm (3.531 eV) beam from a cw argon-ion laser in an external buildup cavity producing ∼100 W of circulating power. Photoelectrons that are ejected perpendicular to the ion and photon beams are collected, energy analyzed by a hemispherical kinetic energy analyzer, and imaged onto a position sensitive detector. The electron energy resolution is typically 7−10 meV full width at half-maximum (fwhm).

Photoelectron spectra are obtained by measuring photoelectron counts as a function of electron kinetic energy (eKE). The energy scale can be converted to electron binding energy (eBE) by subtracting the eKE from the photon energy. The absolute energy scale is calibrated with the EA of atomic oxygen[46] in the measurements of the photoelectron spectra and a linear energy scale compression factor (<1%), which is measured from the photoelectron spectra of reference ions S^-,[47] I^-,[48] and O^- using the EAs of the corresponding atoms. The angle (θ) between the electric field vector of the laser beam and the photoelectron collection axis is controlled with a half-wave plate inserted in the laser beam path. The anisotropy parameter (β), which represents the angular distribution of the photoelectrons, is determined according to eq 1,

$$\beta = \frac{I_{0^\circ} - I_{90^\circ}}{\frac{1}{2} I_{0^\circ} + I_{90^\circ}} \quad (1)$$

where I_{0° and I_{90° are the photoelectron counts at $\theta = 0^\circ$ and $\theta = 90^\circ$, respectively. Spectra measured at the magic angle ($\theta = 54.7^\circ$) are free from angular dependence.

Optimized geometries and harmonic vibrational frequencies (not scaled) for the neutral parent, anion, and radical are determined from density functional theory (DFT) calculations (B3LYP/6-311++G(d,p))[49−51] using the Gaussian 03 suite of programs.[52] Simulated photoelectron spectra were obtained by calculating the Franck−Condon (FC) factors at a vibrational temperature of 300 K with the PESCAL program,[53] using calculated geometries, normal modes, and electron binding energies for the anion and radical. The methyl torsional mode is excluded from the simulation because of the incompatibility with the harmonic assumption used in the simulation.[54]

Flowing Afterglow-Selected Ion Flow Tube (FA-SIFT) Measurements. Gas-phase acidity ($\Delta_{acid}G_{298}$) measurements of *N*-methylpyrazole and *N*-methylimidazole were obtained using a tandem flowing afterglow-selected ion flow tube instrument, FA-SIFT.[55] In this technique, gas-phase acidity measurements of a compound with unknown acidity (AH) are made relative to a reference acid (RH) by determining forward (k_f) and reverse (k_r) proton-transfer reaction rate constants.

$$A^- + RH \underset{k_r}{\overset{k_f}{\rightleftharpoons}} AH + R^- \quad (2)$$

Reactant ions are formed in a flowing afterglow source, mass selected by a quadrupole mass filter, and injected into the reaction flow tube where they are thermalized to ~298 K by collisions with He buffer gas (~0.5 torr, 10^4 cm s^{-1}). Measured flows of neutral reagents are introduced into the reaction flow tube through a manifold of inlets, and the reactant and product ions are analyzed by a quadrupole mass filter coupled to an electron multiplier. Reaction rate constants are determined by changing the position of neutral reagent addition, thereby varying the reaction distance and time, while monitoring the change in reactant ion intensity. The ratio of forward and reverse rate constants gives the proton-transfer equilibrium constant ($K_{eq} = k_f/k_r$) and, hence, the corresponding free-energy change for reaction 2. The gas-phase acidity ($\Delta_{acid}G_{298}$(AH)) is then found from the relation:

$$\Delta_{acid}G_{298}(AH) = \Delta_{acid}G_{298}(RH) + RT \ln K_{eq} \quad (3)$$

where $\Delta_{acid}G_{298}$(RH) is the known acidity for the reference acid and $\Delta_{acid}G_{298}$(AH) is the free-energy change for the heterolytic cleavage of AH → A^- + H^+, where the most acidic proton is removed. The enthalpy of deprotonation ($\Delta_{acid}H_{298}$(AH)) can be found from eq 4 where $\Delta_{acid}S_{298}$(AH), the entropy of deprotonation, is estimated from electronic structure calculations (B3LYP/6-311++G(d,p)).

$$\Delta_{acid}H_{298}(AH) = \Delta_{acid}G_{298}(AH) + T\Delta_{acid}S_{298}(AH) \quad (4)$$

The acidity of *N*-methylpyrazole is determined relative to methanol [$\Delta_{acid}G_{298}(CH_3OH) = 375.5 \pm 0.6$ kcal mol^{-1}],[56] shown in reaction 5, whereas the acidity of *N*-methylimidazole was determined relative to water [$\Delta_{acid}G_{298}(H_2O) = 383.68 \pm 0.02$ kcal mol^{-1}],[56] shown in reaction 6. The photoelectron spectra collected for both isomers suggest that the C5 position is the most acidic site, and therefore, the acidity measurements represent the acidity of the C5−H bond (see discussion below).

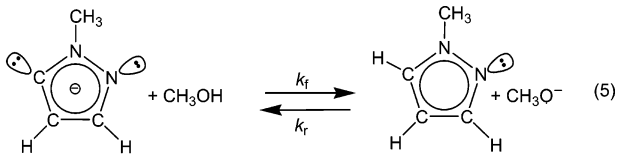

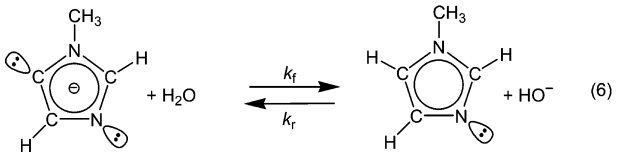

The reactant ions, *N*-methyl-5-pyrazolide, *N*-methyl-5-imidazolide, and CH_3O^-, were formed by proton abstraction from the corresponding neutrals by OH^-, mass selected, and injected into the reaction flow tube with minimal energy to reduce fragmentation from collision-induced dissociation. For all of the reactions studied, with the exception of the reverse reaction of 6, neutral reagent flows were determined by measuring a change in pressure versus time in a calibrated volume; reagents were added to the flow tube through the manifold of inlets. This technique was not used for the reaction of hydroxide with *N*-methylimidazole due to its low volatility. Instead, a regulated but unknown flow of *N*-methylimidazole was introduced into the reaction flow tube at one position. A relative reaction rate was measured by alternately injecting NH_2^- and OH^- for reaction with the constant reactant flow. The neutral reagent concentration and the reaction rate constant were extracted from the relative rate measurement[27,28] by assuming that the highly exothermic proton-transfer reaction of NH_2^- with *N*-methylimidazole proceeds at 90% ± 10% of the calculated collision rate[57] ($k_{col} = 5.7 \times 10^{-9}$ cm^3 s^{-1}).

The forward direction of reaction 5 and the reverse direction of reaction 6 are exothermic, and proton transfer is the only observed pathway. For the corresponding endothermic reactions, adduct formation is observed in addition to proton transfer. The rate constant for proton transfer is determined from the overall rate constant and the proton-transfer branching ratio. An experimental complication in measuring the proton-transfer branching ratio is the occurrence of a secondary switching reaction between the adduct and water.[58] This reaction does not affect the overall rate constant but must be considered in determining the proton-transfer branching ratio. This ratio was measured by monitoring the branching ratio at various reaction times and extrapolating to zero time, where there is no depletion of the adduct due to secondary reaction. Efforts were made to minimize mass discrimination; however, it was necessary to estimate the relative detection sensitivities when calculating the proton-transfer branching ratio. The relative detection sensitivity was estimated by examining a series of exothermic ion−molecule reactions where only one ionic product was formed and the reactant and product ions were similar in mass to the ions of interest (see the Supporting Information).

The absolute uncertainty of each rate constant measurement is generally ±20%, and ±50% for reactions where branching ratios must be evaluated. The absolute error in the gas-phase acidity is smaller because some systematic errors (pressure, temperature, He flow rate, etc.) cancel in the rate ratio. Collision rate constants were calculated from parametrized trajectory collision rate theory.[57,59]

Results and Discussion

Photoelectron Spectra of *N*-Methyl-5-pyrazolide Anion. The 351.1 nm magic-angle photoelectron spectrum of the *N*-methylpyrazolide anion, generated from the reaction of OH^- with *N*-methylpyrazole, is shown in Figure 1a. Electronic structure calculations were used to evaluate the acidity of *N*-methylpyrazole; these results are summarized in Table 1. DFT calculations predict that the C5 carbon is the most acidic site, and therefore, it is most likely that deprotonation by OH^- will occur at this site. Peak a is assigned as the electronic band origin at 2.054 ± 0.006 eV, which corresponds to the EA of the *N*-methyl-5-pyrazolyl radical. The peaks observed at higher eBE correspond to excited vibrational levels of the *N*-methyl-5-pyrazolyl radical. The photoelectron angular distribution was measured and the anisotropy parameter (β) is ~0.5 at the assigned origin but gradually decreases to ~0.1 at 2.8 eV. Beyond 2.8 eV, β rapidly decreases and is −0.4 for peaks l and m.

DFT calculations find minima with C_s symmetry for both the anion and radical. The in-plane CH bond of the methyl group

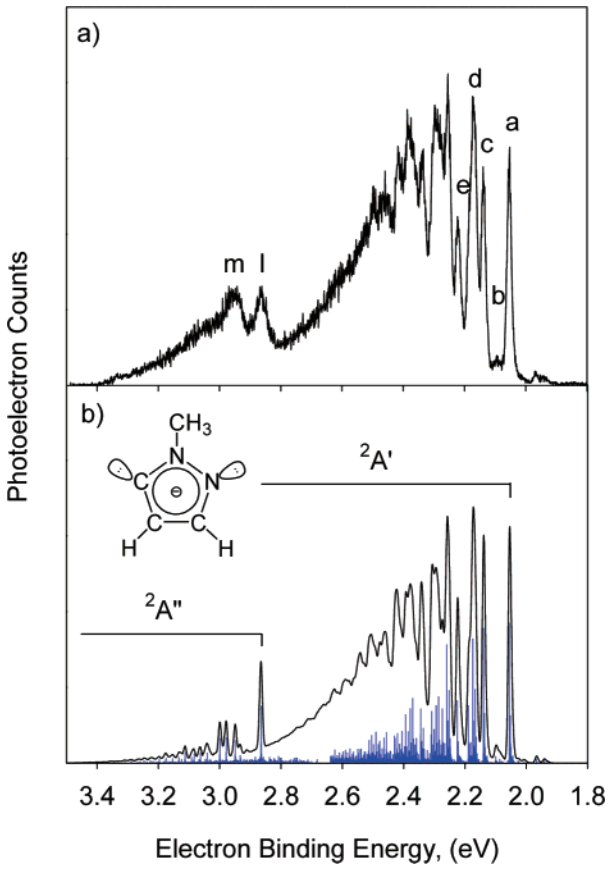

Figure 1. (a) The 351.1 nm magic-angle photoelectron spectrum of the *N*-methyl-5-pyrazolide anion. (b) Simulations of the spectrum based on optimized geometries and normal modes from B3LYP/6-311++G-(d,p) calculations. The sticks (blue) are the raw Franck−Condon (FC) factors, and the solid line is the 10 meV fwhm Gaussian convolutions for transitions from $\tilde{X}^1$A′ *N*-methyl-5-pyrazolide anion to $\tilde{X}^2$A′ and $\tilde{A}^2$A″ *N*-methyl-5-pyrazolyl radical. In the simulated spectra the positions and intensities were set to match those observed in the experimental spectrum.

TABLE 1: B3LYP/6-311++G(d,p) $\Delta_{acid}G_{298}$ and BDE of *N*-Methylpyrazole and *N*-Methylimidazole and the EA of the Corresponding Radicals

		$\Delta_{acid}G_{298}$ (kcal mol^{-1})	EA (eV)	D_0 (kcal mol^{-1})
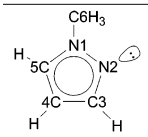		*N-methylpyrazole*		
	C3-H	394.3	1.254	115.5
	C4-H	390.9	1.544	118.8
	C5-H	377.6	2.045	117.5
	C6-H	384.0	0.635	90.9
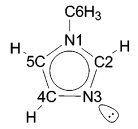		*N-methylimidazole*		
	C2-H	381.7	1.751	114.8
	C4-H	397.9	1.058	115.1
	C5-H	380.8	1.965	118.1
	C6-H	381.0	0.785	91.4

is trans to the N1−N2 bond for both states. The electronic ground state of the *N*-methyl-5-pyrazolide anion is predicted to be $\tilde{X}^1$A′, whereas that of the *N*-methyl-5-pyrazolyl radical is predicted to be $\tilde{X}^2$A′. The calculated EA of the *N*-methyl-5-pyrazolyl radical is 2.045 eV, in good agreement with the assignment of the origin above. DFT calculations predict that there is an excited state, $\tilde{A}^2$A″, with a term energy (T_e) of 0.768 eV. FC factors were computed for the transition from the $\tilde{X}^1$A′ state of the *N*-methyl-5-pyrazolide anion to both the $\tilde{X}^2$A′ and $\tilde{A}^2$A″ states of the *N*-methyl-5-pyrazolyl radical. The stick spectra and the spectrum resulting from convoluting the stick spectrum with a 10 meV fwhm Gaussian function, which represents the instrument resolution, are shown in Figure 1b. The binding energies for both radical states have been slightly shifted (<40 meV) and the intensities normalized to match the experimental spectrum. The simulated spectrum is in excellent agreement with the experimental spectrum and confirms that the spectrum is solely due to the C5 deprotonated anion.

Examination of the DFT optimized geometries (provided in the Supporting Information) shows significant geometry differences between the anion and the ^{2}A′ state of the radical. The most dramatic change is seen in the shortening of the C4−C5 and N1−C5 bonds and the opening of the N1−C5−C4 bond angle. With the use of the FC simulation, several vibrations of the $\tilde{X}^2$A′ state of the *N*-methyl-5-pyrazolyl radical can be assigned. The low-intensity peak b is the fundamental of an in-plane methyl rocking with a frequency of 345 ± 45 cm^{-1}. Peaks c and e are the fundamental and first overtone of an in-plane a′ N2-N1-C5 bend with a frequency of 680 ± 35 cm^{-1}. The three in-plane ring distortion modes (ring bending, N1-N2 stretch, and N1-C5 stretch) contribute to peak d and cannot be resolved within our instrumental resolution. A large number of combination bands of these modes contribute to the spectral features at higher eBE. The atomic displacement for these normal modes, as well as the positions of all the peaks observed in the experimental spectrum, are provided in the Supporting Information. The simulation tends to underestimate the intensity toward the higher eBE, which may be a result of neglecting the methyl torsion levels (explained in the above section). The EA of the *N*-methyl-5-pyrazolyl radical is very close to that of the 5-pyrazolyl radical, 2.104 ± 0.005 eV.[29] Introduction of the methyl group at the N1 position leads to more complication and congestion in the vibronic features, compared to the rather simple, extensive vibrational progression for a ring bending mode observed in the 5-pyrazolide anion spectrum.[29]

The sharp change in β at 2.8 eV is consistent with the presence of another electronic state, seen in the spectrum as peaks l and m. Both peaks l and m have a negative β value, which is distinct from the feature for the $\tilde{X}^2$A′ state where positive β values are found. Positive β values are often observed for low kinetic energy photoelectrons detached from the in-plane orbitals of aromatic systems.[29,60] This is consistent with electron detachment from the C5-centered in-plane (σ) orbital of the $\tilde{X}^1$A′ anion to form the $\tilde{X}^2$A′ radical. In contrast negative β values are often signatures of electrons detached from aromatic π orbitals.[27−29,60] The negative β value for peaks l and m may suggest that the detachment takes place from a π orbital to form the $\tilde{A}^2$A″ state. This observation is consistent with DFT calculations, which find an ^{2}A″ excited state of the *N*-methyl-5-pyrazolyl radical with a calculated T_e of 0.768 eV. The simulated spectrum (shown in Figure 1b at eBE > 2.8 eV) qualitatively resembles the experimental spectrum; however, the observed spectrum is considerably broader than predicted. We attribute the observed broad feature of peaks l and m to the vibronic coupling between the $\tilde{X}^2$A′ and $\tilde{A}^2$A″ states. Vibronic coupling can generate a large number of vibronic levels among which transition intensities are distributed, resulting in broadening.[61] Such broadening has been observed, for instance, in the photoionization of pyrrole.[62] Thus, we conclude that peaks l and m represent the $\tilde{A}^2$A″ vibronic levels, and the T_e is determined to be 0.807 ± 0.009 eV. The EA for the $\tilde{A}^2$A″ state of the *N*-methyl-5-pyrazolyl radical is 2.862 ± 0.007 eV, which is close to the EA of the 1-pyrazolyl radical, 2.938 ± 0.005 eV, where photodetachment takes place from a π orbital of the 1-pyrazolide ion.[29] It should be noted that vibronic coupling

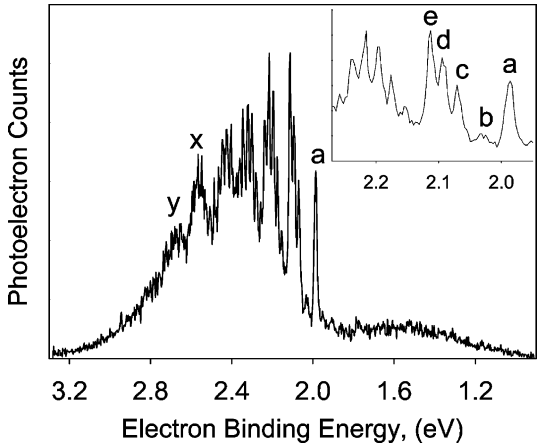

Figure 2. The 351.1 nm magic-angle photoelectron spectrum of the *N*-methylimidazolide anion. A portion of the spectrum near peak a is expanded in the inset.

can also lend some intensity to the highly excited vibronic levels of the $\tilde{X}^2A'$ state, which may explain some of the discrepancy between the observed spectrum and the simulation for the $\tilde{X}^2A'$ state shown in Figure 1b. The observed gradual decrease of the β value toward the higher eBE in the $\tilde{X}^2A'$ spectrum may reflect the nonadiabatic effects.

Photoelectron Spectra of *N*-Methylimidazolide Anion. The 351.1 nm magic-angle photoelectron spectrum of the *N*-methylimidazolide anion is shown in Figure 2. This ion was formed from the reaction of OH^- with *N*-methylimidazole. Analogous to *N*-methylpyrazole, DFT calculations (Table 1) predict that the C5 position is the most acidic site. However, deprotonation by OH^- at the methyl carbon and at the C2 carbon is also exothermic, and therefore, we might expect to see all three isomers in the experimental spectrum. Instead, there appears to be one dominant FC envelope beginning with peak a at 1.987 ± 0.008 eV, an electronic band origin. The photoelectron angular distribution was measured, and β is approximately 0.5 at the origin and smoothly decreases to −0.2 at 3.0 eV. At energies lower than the electronic band origin there are several peaks and a broad band which extends ~1 eV. When the spectrum is collected under cold flow tube conditions (not shown) these lower binding energy peaks are absent, supporting the assignment of the origin.

To aid in the assignment of the experimental spectrum, FC simulations were performed for all three isomeric anions (C5, C2, and methyl anions) and their corresponding ground state neutral radicals. The unadjusted stick spectra and the spectra that result from convoluting the stick spectra with a 10 meV fwhm Gaussian function are shown in Figure 3b−d, along with the experimental spectrum (Figure 3a). It is clear that the spectral features for *N*-imidazolylmethyl anion and the *N*-methyl-2-imidazolide anion are not observed in the experimental spectrum. However, the EA, spectral profile, and even the individual resolved transitions for the *N*-methyl-5-imidazolide anion simulated spectrum are in excellent agreement with the experimental spectrum. Figure 4 shows the lower eBE portion of the C5 anion FC simulation overlaid on the experimental data. In Figure 4 the origin of the simulated spectrum (red trace) has been slightly shifted (<25 meV) to match the experimental data (black trace). This figure further demonstrates that within 300 meV from the origin, where the simulation is most reliable, the predicted relative intensities match the experimental spectrum, confirming that the signal in this region is primarily due to one species. Thus, we conclude that under our experimental conditions deprotonation of *N*-methylimidazole by OH^- almost exclusively occurs at the C5 position.

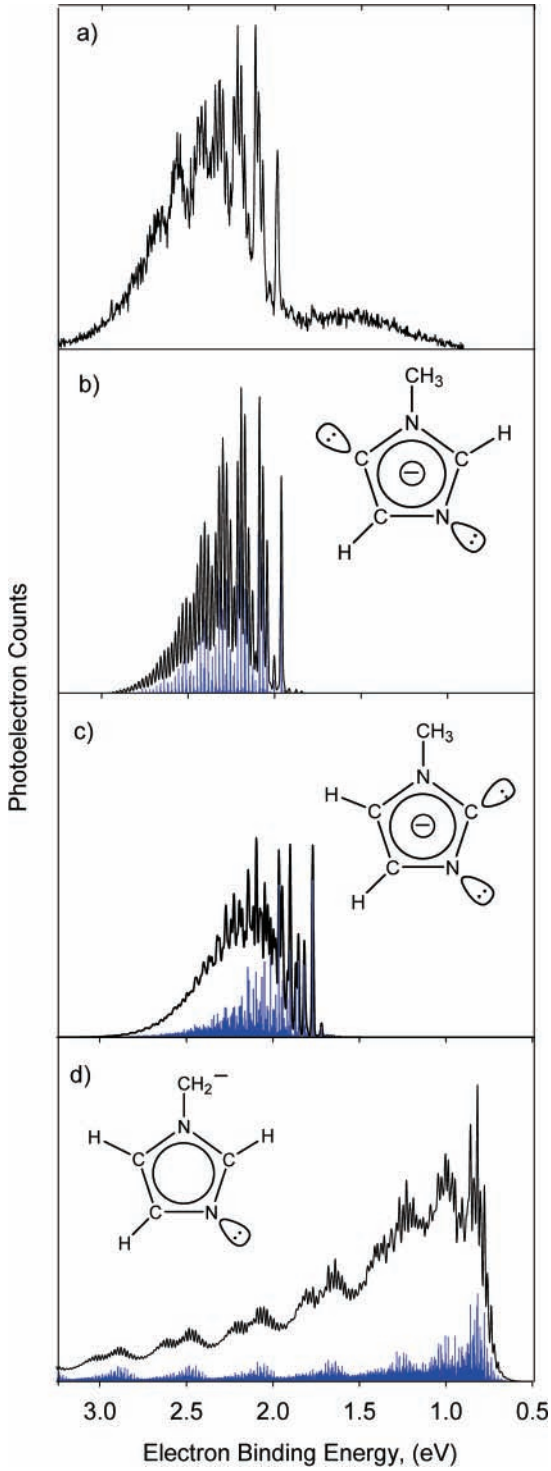

Figure 3. (a) The 351.1 nm magic-angle photoelectron spectrum of the *N*-methylimidazolide anion, reproduced from Figure 2. (b−d) Simulations of the spectrum based on optimized geometries and normal modes from B3LYP/6-311++G(d,p) calculations. The sticks (blue) are the raw Franck−Condon (FC) factors, and the solid line is the 10 meV fwhm Gaussian convolutions for transitions of (b) $\tilde{X}^1A'$ *N*-methyl-5-imidazolide to $\tilde{X}^2A'$ *N*-methyl-5-imidazolyl, (c) $\tilde{X}^1A'$ *N*-methyl-2-imidazolide to $\tilde{X}^2A'$ *N*-methyl-2-imidazolyl, and (d) $\tilde{X}^1A$ *N*-imidazolylmethyl anion to $\tilde{X}^2A'$ *N*-imidazolylmethyl radical.

The calculated EA of the *N*-methyl-5-imidazolyl radical is 1.965 eV, which is close to the assigned origin (peak a). With the use of the FC simulation, four vibrations of the $\tilde{X}^2A'$ state

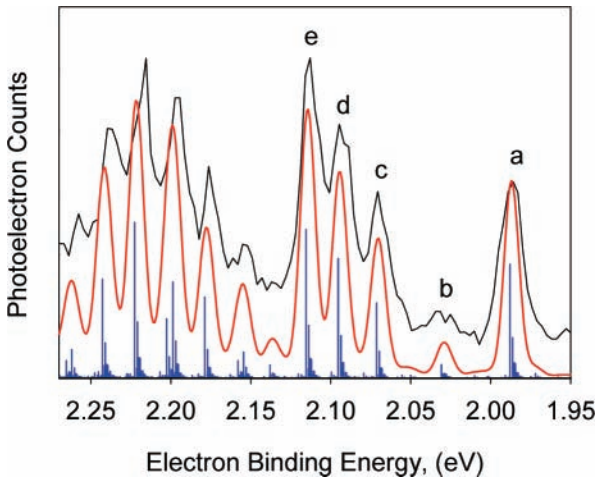

Figure 4. The 351.1 nm magic-angle photoelectron spectrum of the *N*-methylimidazolide anion (black), reproduced from Figure 2, and the simulated 10 meV Gaussian convoluted (red) and stick (blue) spectra, reproduced from Figure 3b. The eBE of the origin for the simulated spectra was set to match the eBE of peak a in the experimental spectrum.

of the *N*-methyl-5-imidazolyl radical can be assigned. The small intensity peak b is assigned to a methyl rocking mode with a frequency of 345 ± 30 cm^{-1}. Peaks c, d, and e are partially resolved fundamentals of in-plane ring distortion modes. Peak c corresponds to a C2-N1-C5 bend with a frequency of 675 ± 25 cm^{-1}, peak d to a C2-N3-C4 bend with a frequency of 865 ± 35 cm^{-1}, and peak e to a C4-C5-N1 bend with a frequency of 1015 ± 25 cm^{-1}. Combination bands of these modes are observed in the larger eBE region. The atomic displacements for these normal modes along with the experimental peak positions are provided in the Supporting Information. The same bending modes are active in the photoelectron spectrum of the 5-imidazolide anion spectrum, and the EA of the *N*-methyl-5-imidazolyl radical is very close to that of the 5-imidazolyl radical, 1.992 ± 0.010 eV.[27]

Following the analysis of the *N*-methyl-5-pyrazolide anion spectrum, we consider photodetachment to the $\tilde{A}^2A''$ state of the *N*-methyl-5-imidazolyl radical. DFT calculations predict the T_e be 0.452 eV.[63] This T_e corresponds to the broad band x in Figure 2. Analogous to the *N*-methyl-5-pyrazolyl radical system, vibronic coupling between the $\tilde{X}^2A'$ and $\tilde{A}^2A''$ states is expected for the *N*-methyl-5-imidazolyl radical, which can broaden the spectral profile. In the previous section, we noted the similarity between the eBE for the detachment to the $\tilde{A}^2A''$ state of *N*-methyl-5-pyrazolyl and the EA of the 1-pyrazolyl radical. In this sense, because the EA of the 1-imidazolyl radical is 2.613 ± 0.006 eV,[27] the broad band y in Figure 2 seems to correspond to the vibrational origin of the $\tilde{A}^2A''$ *N*-methyl-5-imidazolyl radical. Rigorous assignment is impossible in the present study, but it is most likely that some of the spectral features at eBE > 2.4 eV represents the $\tilde{A}^2A''$ state of the radical. Gradual decrease of the β value toward the higher eBE is consistent with this conclusion. The broad background at eBE > 2.0 eV may be a manifestation of the nonadiabatic effects as well.

As mentioned above, deprotonation of *N*-methylimidazole at the methyl and C2 sites by hydroxide is predicted to be exothermic. Nonetheless the spectral features for these two anions are absent in the experimental spectrum, suggesting that these isomers are not formed in any significant amounts. This notion, however, should be taken with caution, because the identity of the low-intensity, broad feature observed at eBE < 2.0 eV is uncertain. This feature is absent when the ions are synthesized in a flow tube cooled with liquid nitrogen. There may be an isomerization process (e.g., ring-opening) when OH^- interacts with a H atom at C2, C4, or the methyl group.

Gas-Phase Acidity of *N*-Methylpyrazole. The gas-phase acidity of *N*-methylpyrazole was measured relative to methanol[56] (shown in reaction 5). For the forward reaction, the *N*-methylpyrazolide anion is prepared from a proton-transfer reaction of *N*-methylpyrazole with OH^- in the source. The photoelectron spectrum of *N*-methylpyrazolide, where the anion was prepared from proton transfer to hydroxide, shows that deprotonation only occurs on the C5 site. The forward reaction of the *N*-methyl-5-pyrazolide anion with CH_3OH is exothermic, and the reaction proceeds exclusively by proton transfer. The rate constant is measured to be 1.3 ± 0.1 × 10^{-9} cm^3 s^{-1} (0.68 efficiency). The reverse reaction of CH_3O^- with *N*-methylpyrazole is endothermic, and significant adduct formation is observed in addition to proton transfer. The overall rate constant is 5.5 ± 0.4 × 10^{-10} cm^3 s^{-1} (0.19 efficiency). The proton-transfer rate constant was determined from the overall rate constant and the proton-transfer branching ratio to be 1.2 ± 0.3 × 10^{-10} cm^3 s^{-1}.

Combining the forward and reverse proton-transfer rate constants, the gas-phase acidity ($\Delta_{acid}G_{298}$) of *N*-methylpyrazole is determined to be 376.9 ± 0.7 kcal mol^{-1}, which is in exact agreement with the calculated value. The DFT entropy of deprotonation, $\Delta_{acid}S_{298}$ = 23.7 cal mol^{-1} K^{-1}, is used with $\Delta_{acid}G_{298}$ to calculate the enthalpy of deprotonation ($\Delta_{acid}H_{298}$) to be 384.0 ± 0.7 kcal mol^{-1}.

Gas-Phase Acidity of *N*-Methylimidazole. The gas-phase acidity of *N*-methylimidazole was measured relative to water (shown in eq 6). In both the forward and reverse reactions the *N*-methylimidazolide anion is formed from deprotonation of the neutral by OH^-. (For the forward reaction this step occurs in the source.) As discussed in the analysis of the *N*-methylimidazolide anion photoelectron spectrum, deprotonation of *N*-methylimidazole by OH^- almost exclusively occurs at the C5 site. If the methyl and C2 isomers are present they are in minor amounts and therefore would not significantly affect the experimental gas-phase acidity value.

The forward reaction of the *N*-methylimidazolide anion with H_2O is endothermic, and significant adduct formation is observed in addition to proton transfer. The overall rate constant is found to be 1.0 ± 0.3 × 10^{-10} cm^3 s^{-1} (0.04 efficiency). Kinetic plots for this reaction were measured as a function of SIFT injection potential (over a 50 V range) and are observed to be linear, which supports the conclusion that other isomeric ions are not present in significant amounts. The proton-transfer rate constant is determined from the overall rate constant and the proton-transfer branching ratio to be 1.3 ± 0.3 × 10^{-11} cm^3 s^{-1}. The reverse reaction of OH^- with *N*-methylimidazole is exothermic, and proton transfer is the only reaction pathway observed. The proton-transfer reaction rate constant was determined relative to that for the reaction of *N*-methylimidazole with NH_2^-, which is highly exothermic, assuming that this reaction proceeds at 90% ± 10% of the collision rate. This assumption is validated by measurements of the proton-transfer rate constant for the reaction of NH_2^- with *N*-methylpyrazole, which is slightly more exothermic and found to occur at the collision rate. The proton-transfer rate constant for *N*-methylimidazole with OH^- is determined to be 4.6 ± 0.5 × 10^{-9} cm^3 s^{-1} (0.82 efficiency).

With the use of eq 3, $\Delta_{acid}G_{298}$ is determined to be 380.2 ± 1.0 kcal mol^{-1}. Although the gas-phase acidity of H_2O is known to within ± 0.02 kcal mol^{-1}, we have assigned more conserva-

tive error bars to the gas-phase acidity of *N*-methylimidazole to account for the possibility that another, more basic isomer may be present.[64] The experimental gas-phase acidity is in good agreement with the calculated value of 380.8 kcal mol^{-1}. The DFT calculated $\Delta_{acid}S_{298} = 26.5$ cal mol^{-1} K^{-1}; therefore, using eq 4, $\Delta_{acid}H_{298}$ is determined to be 388.1 ± 1.0 kcal mol^{-1}.

H/D Exchange of *N*-Methylimidazolide Anion. The observation that deprotonation of *N*-methylimidazole by OH^- results in almost exclusively the C5 anion has prompted us to investigate the H/D exchange reaction of the *N*-methylimidazolide anion with D_2O and ND_3. H/D exchange experiments have proven to be a useful probe for determining anion structures and for studies of the structure and dynamics of ion−dipole complexes.[65] In this process, the ion and deuterated reagent enter a long-lived complex, which typically contains ∼15−20 kcal mol^{-1} excess energy.[65] During the lifetime of this ion−dipole complex, proton−deuteron scrambling can occur before the ion and neutral separate.

D_2O and ND_3 are useful exchange reagents in that they can both exchange more than one deuteron in an encounter. These two exchange reagents differ from one another in that ion−molecule complexes with ND_3 typically contain less energy than ion−molecule complexes with D_2O.[66] When *N*-methylimidazolide anion is allowed to react with ND_3 four exchanges are observed. Assuming that the initial anionic site is at the C5 position, three exchanges are due to the methyl group and one exchange is from a ring proton (either C2 or C4 protons). The first step of the exchange, the deuteron transfer reaction of *N*-methyl-5-imidazolide anion with ND_3, is sufficiently endothermic (∼15 kcal mol^{-1}) and consumes almost all of the complexation energy. With the use of the DFT calculated acidities as a guide (Table 1), back-transfer of a proton to ND_2^- from the methyl or C2 position is energetically favored, whereas proton transfer from the C4 position would consume an additional ∼2 kcal mol^{-1} of the complexation energy. Any subsequent exchange, therefore, is most likely to occur at the methyl or C2 position. When D_2O is used as an exchange reagent four exchanges are also observed. Despite the fact that ion−molecule complexes with D_2O have larger excess energy than complexes with ND_3 and that the initial deuteron transfer is less endothermic, exchange at the C4 position is not observed. These results are consistent with computations, which predict that the C4 proton is significantly less acidic than other sites in the molecule. Furthermore, these results indicate that the methyl and C2 positions are accessible.

Thermochemistry of *N*-Methylpyrazole and *N*-Methylimidazole. The C5−H BDE (D_0) of *N*-methylpyrazole and *N*-methylimidazole can be determined from the EA measurements and the enthalpy of deprotonation using a negative ion thermochemical cycle.[33,34]

$$D_0(\mathrm{AH}) = \Delta_{acid}H_0(\mathrm{AH}) + \mathrm{EA(A)} - \mathrm{IE(H)} \quad (7)$$

Here, $\Delta_{acid}H_0$(AH) is the C5−H deprotonation enthalpy of the *N*-methylazole at 0 K, EA(A) is the electron affinity of the *N*-methylazolyl radical, and IE(H) is the ionization energy of the hydrogen atom (13.59844 eV).[66] A thermal correction (∼1.4 kcal mol^{-1}) is applied to convert the 298 K enthalpy of deprotonation to 0 K (eq 8); the integrated heat capacities are found from DFT calculations.

$$\Delta_{acid}H_0(\mathrm{AH}) = \Delta_{acid}H_{298}(\mathrm{AH}) - \int_0^{298} [C_p(\mathrm{A}^-) + C_p(\mathrm{H}^+) - C_p(\mathrm{AH})]\,dT \quad (8)$$

TABLE 2: Thermochemical Parameters

N-methylpyrazole and *N*-methyl-5-pyrazolyl radical	
EA(*N*-methyl-5-pyrazolyl)[a]	2.054 ± 0.006 eV
T_e(*N*-methyl-5-pyrazolyl)[a]	0.807 ± 0.009 eV
$\Delta_{acid}G_{298}$(C5−H, *N*-methylpyrazole)[a]	376.9 ± 0.7 kcal mol^{-1}
$\Delta_{acid}S_{298}$(C5−H, *N*-methylpyrazole)[b]	23.7 cal mol^{-1} K^{-1}
$\Delta_{acid}H_{298}$(C5−H, *N*-methylpyrazole)[c]	384.0 ± 0.7 kcal mol^{-1}
$\Delta_{acid}H_0$(C5−H, *N*-methylpyrazole)[d]	382.6 ± 0.7 kcal mol^{-1}
D_0(C5−H, *N*-methylpyrazole)[e]	116.4 ± 0.7 kcal mol^{-1}
Δ_fH_{298}(*N*-methylpyrazole)[f]	103.1 ± 1.5 kcal mol^{-1}
N-methylimidazole and *N*-methyl-5-imidazolyl radical	
EA(*N*-methyl-5-imidazolyl)[a]	1.987 ± 0.008 eV
$\Delta_{acid}G_{298}$(C5−H, *N*-methylimidazole)[a]	380.2 ± 1.0 kcal mol^{-1}
$\Delta_{acid}S_{298}$(C5−H, *N*-methylimidazole)[b]	26.5 cal mol^{-1} K^{-1}
$\Delta_{acid}H_{298}$(C5−H, *N*-methylimidazole)[c]	388.1 ± 1.0 kcal mol^{-1}
$\Delta_{acid}H_0$(C5−H, *N*-methylimidazole)[d]	386.8 ± 1.1 kcal mol^{-1}
D_0(C5−H, *N*-methylimidazole)[e]	119.0 ± 1.0 kcal mol^{-1}
Δ_fH_{298}(*N*-methylimidazole)[f]	101.2 ± 3.1 kcal mol^{-1}

[a] Experimentally determined in this study. [b] Determined from B3LYP/6-311++G(d,p) calculations. [c] Calculated from $\Delta_{acid}G_{298}$ and $\Delta_{acid}S_{298}$ (see eq 4 in text). [d] Calculated from $\Delta_{acid}H_{298}$ (see eq 8 in text). [e] Calculated using the EA and $\Delta_{acid}H_0$ in addition to the IE(H) (see eq 7 in text). [f] Calculated from Δ_fH_{298}(H), Δ_fH_{298}(RH), and D_{298}(RH) (see eqs 9 and 10 in text).

In *N*-methylpyrazole, where the two nitrogen atoms are adjacent, the D_0(C5−H) is determined to be 116.4 ± 0.7 kcal mol^{-1}. In *N*-methylimidazole, where the two nitrogen atoms are separated by one carbon atom, the D_0(C5−H) is determined to be 119.0 ± 1.0 kcal mol^{-1}. The uncertainty in the BDE measurements is largely due to the error in the gas-phase acidity measurements. Table 2 summarizes these BDEs as well as other thermodynamic values reported in this work. The BDE is the energy required to break the C−H bond to form the radical and an H atom. The difference in the BDE of the two isomers is 2.6 kcal mol^{-1}, indicating that the location of the remote (β position) nitrogen atom in the ring does not significantly change the strength of the C5−H bond. This subtle difference, however, does indicate that the *N*-methyl-5-pyrazolyl radical is slightly more stable than the *N*-methyl-5-imidazolyl radical relative to their respective neutral azoles. Similarly, gas-phase acidity measurements indicate that the *N*-methyl-5-pyrazolide anion is more stable than the *N*-methyl-5-imidazolide anion when compared to the corresponding neutral azoles.

The heat of formation of the *N*-methylazolyl radicals, Δ_fH_{298}(A), can be determined from the BDE of the *N*-methylazoles using eq 9.

$$\Delta_fH_{298}(\mathrm{A}) = D_{298}(\mathrm{AH}) + \Delta_fH_{298}(\mathrm{AH}) - \Delta_fH_{298}(\mathrm{H}) \quad (9)$$

Here D_{298}(AH) is the BDE of the *N*-methylazole at 298 K, Δ_fH_{298}(H) is the heat of formation of hydrogen (52.103 ± 0.001 kcal mol^{-1})[67] and Δ_fH_{298}(AH) is the heat of formation of the *N*-methylazole (Δ_fH_{298}(*N*-methylpyrazole) = 37.4 ± 0.5 kcal mol^{-1} and Δ_fH_{298}(*N*-methylimidazole) = 32.9 ± 1.0 kcal mol^{-1}.[68] Again a small thermal correction, shown in eq 10, is needed to bring the BDE of AH from 0 to 298 K.

$$D_{298}(\mathrm{AH}) = D_0(\mathrm{AH}) + \int_0^{298} [C_p(\mathrm{A}) + C_p(\mathrm{H}) - C_p(\mathrm{AH})]\,dT \quad (10)$$

The heat of formation is determined to be 103.1 ± 1.5 kcal mol^{-1} for the *N*-methyl-5-pyrazolyl radical and 101.2 ± 3.1 kcal mol^{-1} for the *N*-methyl-5-imidazolyl radical.

If the methyl group does not significantly change the C−H bond energetics, the thermochemical properties measured here should be consistent with those of pyrazole and imidazole. For

imidazole, the previously measured C5−H bond strength (119 ± 4 kcal mol^{-1}) is similar to the value reported here for *N*-methylimidazole (118.1 ± 1.0 kcal mol^{-1}), which has much greater precision. In addition, the EA and gas-phase acidity reported here are also similar to those for imidazole ($\Delta_{acid}G_{298}$(C5−H, imidazole) = 380 ± 4 kcal mol^{-1}, EA(5-imidazolyl) = 1.992 ± 0.010 eV).[27] The previously measured bond strength of pyrazole (121 ± 4 kcal mol^{-1}), on the other hand, is 4.6 kcal mol^{-1} higher than the value reported here for *N*-methylpyrazole. The difference in bond strength is primarily due to the difference in the measured acidity, 4 kcal mol^{-1} ($\Delta_{acid}G_{298}$(C5−H, pyrazole) = 380 ± 4 kcal mol^{-1}, EA(5-pyrazolyl) = 2.104 ± 0.005 eV). It seems unlikely that the substitution of a methyl group on pyrazole would significantly perturb the energetics of the C−H bonds, especially since there is no significant effect for *N*-methylimidazole. More likely it seems that the difference in BDEs of pyrazole and *N*-methylpyrazole reflects the difficulties in determining the C5−H acidity of pyrazole.[69] Thus, the C5−H BDE values reported in this work, at the present time, represent the most accurate C−H BDE values for the family of azoles.

The C5−H BDEs of *N*-methylpyrazole and *N*-methylimidazole determined in this work are significantly larger than the C−H BDE of benzene (D_0(C−H) = 112.0 ± 0.6 kcal mol^{-1}), a benchmark C−H bond strength for aromatic compounds.[70] Generally, C−H BDEs in five-membered ring aromatic compounds are predicted theoretically to be larger than those in six-membered aromatics; this has been discussed with respect to the difference in the molecular structure.[12] The inherently smaller interior angle in a five-membered ring makes the corresponding C−H bond stronger because the 2s orbital of the C atom contributes more to the C−H bonding orbital. While our experimental findings are consistent with this argument, the reported C−H BDE of another five-membered ring compound, the cyclopentadienyl radical (C_5H_5),[71] D_{298} = 105.0 ± 3.4 kcal mol^{-1}, is much lower than the C5−H BDEs of the *N*-methylazoles and the C−H BDE of benzene. In this case, however, the cyclopentadienyl radical is not a $4n + 2$ Hückel system.[72] Following C−H bond fission, the resultant cyclopentadienylidene would maintain an unpaired electron in the π (b1) orbital in the electronic ground state ($^3B_1$), inducing a static Jahn−Teller stabilization, which may explain the low C−H BDE of the cyclopentadienyl radical.

In order to extend the knowledge of the C−H BDEs of azoles, we are currently investigating *N*-methylpyrrole. It is difficult, however, to determine the C2−H BDE (which is equivalent to the C5−H BDE by symmetry) using the same experimental technique employed in this study, because N-methylation of pyrrole does not make the C2 carbon the most acidic location.[73] The C2−H BDE of pyrrole has been reported to be 112.5 ± 1 kcal mol^{-1} according to a photofragment translational spectroscopic study.[23] It should be mentioned, however, that more recent studies[24,25] have not observed a C−H bond dissociation process in the photochemistry of pyrrole. In light of the discrepancy in the N−H BDE of pyrrole, there are some questions about the reported C2−H BDE of pyrrole in the aforementioned study. It should also be noted that a photofragment velocity map imaging technique has been ineffective to explore the C−H BDE of *N*-methylpyrrole.[24] Our study on the C2−H BDE of *N*-methylpyrrole will be presented in a forthcoming paper.[74]

Conclusion

The 351.1 nm photoelectron spectrum of the *N*-methyl-5-pyrazolide anion was measured and is in excellent agreement with the calculated FC factors for the transition from the $\tilde{X}^1A'$ state of the anion to the $\tilde{X}^2A'$ and $\tilde{A}^2A''$ states of the *N*-methyl-5-pyrazolyl radical. The EA of the radical is 2.054 ± 0.006 eV, and the T_e of the $\tilde{A}^2A''$ state is 0.807 ± 0.009 eV. Fundamental vibrational frequencies of 345 ± 45 and 680 ± 35 cm^{-1} are found for an in-plane methyl rocking and C5-N1-N2 bending modes of the $\tilde{X}^2A'$ state of the *N*-methyl-5-pyrazolyl radical, respectively. The gas-phase acidity of *N*-methylpyrazole was measured relative to methanol, $\Delta_{acid}G_{298}$(*N*-methylpyrazole) = 376.9 ± 0.7 kcal mol^{-1} and $\Delta_{acid}H_{298}$(*N*-methylpyrazole) = 384.0 ± 0.7 kcal mol^{-1}. With the use of a negative ion thermodynamic cycle the C5−H BDE was determined to be D_0(*N*-methylpyrazole) = 116.4 ± 0.7 kcal mol^{-1} and Δ_fH_{298}(*N*-methylpyrazole) = 103.1 ± 1.5 kcal mol^{-1}.

The 351.1 nm photoelectron spectrum of the *N*-methyl-5-imidazolide anion was measured and is in good agreement with the calculated FC factors for the $\tilde{X}^1A'$ state of the anion to the $\tilde{X}^2A'$ state of the *N*-methyl-5-imidazolyl radical. The EA of the radical is 1.987 ± 0.008 eV. Fundamental frequencies of four in-plane modes are 345 ± 30 cm^{-1} (methyl rocking), 675 ± 25 cm^{-1} (C5-N1-C2), 865 ± 35 cm^{-1} (C2-N3-C4), and 1015 ± 25 cm^{-1} (C4-C5-N1) for the $\tilde{X}^2A'$ state of the *N*-methyl-5-imidazolyl radical. The gas-phase acidity of *N*-methylimidazole was measured relative to water, $\Delta_{acid}G_{298}$(*N*-methylimidazole) = 380.2 ± 1.0 kcal mol^{-1} and $\Delta_{acid}H_{298}$(*N*-methylimidazole) = 388.1 ± 1.0 kcal mol^{-1}. With the use of a negative ion thermodynamic cycle the C5−H BDE and the heat of formation of the *N*-methyl-5-imidazolyl radical were determined to be 119.0 ± 1.0 kcal mol^{-1} and 101.2 ± 3.1 kcal mol^{-1}, respectively.

Acknowledgment. We dedicate this paper to Prof. Charles H. DePuy on the occasion of his 80th birthday, and we thank him for his valuable comments. We are also grateful to Mr. Todd B. Kreutzian for determining the water content of the neutral reagents and Prof. Paul G. Wenthold and Prof. Jeehiun K. Lee for sharing their unpublished work with us. This work is supported by the AFOSR (FA9550-06-1-006). In addition, W.C.L. acknowledges support from NSF (CHE0512188 and PHY0551010) and V.M.B. acknowledges NSF (CHE0349937).

Supporting Information Available: The B3LYP/6-311++G(d,p) optimized geometries and thermochemical values of *N*-methylpyrazole, *N*-methyl-5-pyrazolide anion, *N*-methyl-5-pyrazolyl radical, *N*-methylimidazole, *N*-methyl-5-imidazolide anion, and *N*-methyl-5-imidazolyl radical; harmonic vibrational frequencies for the above anions and radicals; a more complete list of the experimental peak positions for the *N*-methyl-5-pyrazolide anion and the *N*-methyl-5-imidazolide anion spectra; normal mode displacements for the active vibrations of $\tilde{X}^2A'$ state of the *N*-methyl-5-pyrazolyl radical and $\tilde{X}^2A'$ state of the *N*-methyl-5-imidazolyl radical; an explanation of the mass discrimination estimate. This material is available free of charge via the Internet at http://pubs.acs.org.

References and Notes

(1) Abeles, R. H.; Frey, P. A.; Jencks, W. P. *Biochemistry*, 1st ed.; Jones and Bartlett: Boston, MA, 1992.
(2) Toribio, L.; Nozal, N. M. J.; Bernal, J.; Alonso, C.; Jimenez, J. L. *J. Chromatogr., A* **2007**, *1144*, 255.
(3) Ahmad, Z.; Sharma, S.; Khuller, G. K. *FEMS Microbiol. Lett.* **2006**, *261*, 181.
(4) Ogihara, W.; Yoshizawa, M.; Ohno, H. *Chem. Lett.* **2004**, *33*, 1022.
(5) Jorapur, Y. R.; Jeong, J. M.; Chi, D. Y. *Tetrahedron Lett.* **2006**, *47*, 2435.
(6) Raposo, M. M. M.; Sousa, A. M. R. C.; Fonseca, A. M. C.; Kirsch, G. *Adv. Mater. Forum III, Parts 1 and 2* **2006**, *103*, 514.

(7) Zhao, W.; Carreira, E. M. *Chem. Eur. J.* **2006**, *12*, 7254.
(8) Williams, G. K.; Palopoli, S. F.; Brill, T. B. *Combust. Flame* **1994**, *98*, 197.
(9) Knicker, H.; Hatcher, P. G.; Scaroni, A. W. *Energy Fuels* **1995**, *9*, 999.
(10) Okumara, Y.; Sugiyama, Y.; Okazaki, K. *Fuel* **2002**, *81*, 2317.
(11) Snyder, L. R. *Anal. Chem.* **1969**, *41*, 314.
(12) Barckholtz, C.; Barckholtz, T. A.; Hadad, C. M. *J. Am. Chem. Soc.* **1999**, *121*, 491.
(13) Shapley, J. R.; Samkoff, D. E.; Bueno, C.; Churchill, M. R. *Inorg. Chem.* **1982**, *21*, 634.
(14) Jones, W. D.; Dong, L. Z.; Myers, A. W. *Organometallics* **1995**, *14*, 855.
(15) Agarwala, R.; Azam, K. A.; Dilshad, R.; Kabir, S. E.; Miah, R.; Shahiduzzaman, M.; Hardcastle, K. I.; Rosenberg, E.; Hursthouse, M. B.; Abdul Malik, K. M. *J. Organomet. Chem.* **1995**, *492*, 135.
(16) Musaev, D. G.; Morokuma, K. *J. Am. Chem. Soc.* **1995**, *117*, 799.
(17) Xie, K. C.; Lin, J. Y.; Li, W. Y.; Chang, L. P.; Feng, J.; Zhao, W. *Fuel* **2005**, *84*, 271.
(18) Babich, I. V.; Seshan, K.; Lefferts, L. *Appl. Catal., B* **2005**, *59*, 205.
(19) Mackie, J. C.; Colket, M. B.; Nelson, P. F.; Esler, M. *Int. J. Chem. Kinet.* **1991**, *23*, 733.
(20) Lifshitz, A.; Tamburu, C.; Suslensky, A. *J. Phys. Chem.* **1989**, *93*, 5802.
(21) Dubnikova, F.; Lifshitz, A. *J. Phys. Chem. A* **1998**, *102*, 10880.
(22) Mackie, J. C.; Colket, M. B.; Nelson, P. F. *J. Phys. Chem.* **1990**, *94*, 4099.
(23) Blank, D. A.; North, S. W.; Lee, Y. T. *Chem. Phys.* **1994**, *187*, 35.
(24) Wei, J.; Kuczmann, A.; Riedel, J.; Renth, F.; Temps, F. *Phys. Chem. Chem. Phys.* **2003**, *5*, 315.
(25) Cronin, B.; Nix, M. G. D.; Qadiri, R. H.; Ashfold, M. N. R. *Phys. Chem. Chem. Phys.* **2004**, *6*, 5031.
(26) Kiefer, J. H.; Zhang, Q.; Kern, R. D.; Yao, J.; Jursic, B. *J. Phys. Chem. A* **1997**, *101*, 7061.
(27) Gianola, A. J.; Ichino, T.; Hoenigman, R. L.; Kato, S.; Bierbaum, V. M.; Lineberger, W. C. *J. Phys. Chem. A* **2005**, *109*, 11504.
(28) Gianola, A. J.; Ichino, T.; Hoenigman, R. L.; Kato, S.; Bierbaum, V. M.; Lineberger, W. C. *J. Phys. Chem. A* **2004**, *108*, 10326.
(29) Gianola, A. J.; Ichino, T.; Kato, S.; Bierbaum, V. M.; Lineberger, W. C. *J. Phys. Chem. A* **2006**, *110*, 8457.
(30) Ichino, T.; Gianola, A. J.; Lineberger, W. C.; Stanton, J. F. *J. Chem. Phys.* **2006**, *125*, 084312.
(31) Ichino, T.; Andrews, D. H.; Rathbone, G. J.; Misaizu, F.; Calvi, R. M. D.; Wren, S. W.; Kato, S.; Bierbaum, V. M.; Lineberger, W. C. Submitted to *J. Phys. Chem. A.*
(32) Ervin, K. M.; Lineberger, W. C. In *Gas Phase Ion Chemistry*; Adams, N. C., Babcock, L. M., Eds.; JAI Press: Greenwich, CT, 1992; Vol. 1, p 121.
(33) Blanksby, S. J.; Ellison, G. B. *Acc. Chem. Res.* **2003**, *36*, 255.
(34) Berkowitz, J.; Ellison, G. B.; Gutman, D. *J. Phys. Chem.* **1994**, *98*, 2744.
(35) O'Hair, R. A. J.; Gronert, S.; DePuy, C. H.; Bowie, J. H. *J. Am. Chem. Soc.* **1989**, *111*, 3105.
(36) Hare, M. C.; Marimanikkuppam, S. S.; Kass, S. R. *Int. J. Mass Spectrom.* **2001**, *210*, 153.
(37) Baschky, M. C.; Peterson, K. C.; Kass, S. R. *J. Am. Chem. Soc.* **1994**, *116*, 7218.
(38) Chou, P. K.; Kass, S. R. *J. Am. Chem. Soc.* **1991**, *113*, 4357.
(39) Wenthold, P. G.; Squires, R. R. *J. Am. Chem. Soc.* **1994**, *116*, 6401.
(40) Grabowski, J. J.; Cheng, X. H. *J. Am. Chem. Soc.* **1989**, *111*, 3106.
(41) Kurinovich, M. A.; Lee, J. K. *J. Am. Chem. Soc.* **2000**, *122*, 6258.
(42) Sharma, S.; Lee, J. K. *J. Org. Chem.* **2002**, *67*, 8360.
(43) Leopold, D. G.; Murray, K. K.; Miller, A. E. S.; Lineberger, W. C. *J. Chem. Phys.* **1985**, *83*, 4849.
(44) Ervin, K. M.; Ho, J.; Lineberger, W. C. *J. Chem. Phys.* **1989**, *91*, 5974.
(45) Wenthold, P. G.; Polak, M. L.; Lineberger, W. C. *J. Phys. Chem.* **1996**, *100*, 6920.
(46) Neumark, D. M.; Lykke, K. R.; Andersen, T.; Lineberger, W. C. *Phys. Rev. A: At., Mol., Opt. Phys.* **1985**, *32*, 1890.
(47) Hotop, H.; Lineberger, W. C. *J. Phys. Chem. Ref. Data* **1985**, *14*, 731.
(48) Hanstorp, D.; Gustafsson, M. *J. Phys. B: At. Mol. Opt. Phys.* **1992**, *25*, 1773.
(49) Becke, A. D. *J. Chem. Phys.* **1993**, *98*, 5648.
(50) Lee, C. T.; Yang, W. T.; Parr, R. G. *Phys. Rev. B: Condens. Matter* **1988**, *37*, 785.
(51) Krishnan, R.; Binkley, J. S.; Seeger, R.; Pople, J. A. *J. Chem. Phys.* **1980**, *72*, 650.
(52) Frisch, M. J.; Trucks, G. W.; Schlegel, H. B.; Scuseria, G. E.; Robb, M. A. et al. *Gaussian 03*, revision B.05; Gaussian, Inc.: Pittsburgh, PA, 2003.
(53) Ervin, K. M.; Ramond, T. M.; Davico, G. E.; Schwartz, R. L.; Casey, S. M.; Lineberger, W. C. *J. Phys. Chem. A* **2001**, *105*, 10822.
(54) The B3LYP/6-311++G(d,p) calculations predict that the threefold barriers for the methyl torsion are 247 and 105 cm^{-1} for *N*-methyl-5-pyrazolide and *N*-methyl-5-pyrazolyl, respectively. They are 47 and 111 cm^{-1} for *N*-methyl-5-imidazolide and *N*-methyl-5-imidazolyl, respectively.
(55) Van Doren, J. M.; Barlow, S. E.; DePuy, C. H.; Bierbaum, V. M. *Int. J. Mass Spectrom. Ion Processes* **1987**, *81*, 85.
(56) Ervin, K. M.; DeTuro, V. F. *J. Phys. Chem. A* **2002**, *106*, 9947.
(57) Su, T.; Chesnavich, W. J. *J. Chem. Phys.* **1982**, *76*, 5183.
(58) For the reverse direction in reaction (5) water was present in trace amounts in the *N*-methylpyrazole sample. The amount of water contained in the neutral reagent was determined by Carl Fisher titration to be 1.48 wt %; however, the percent of water in the vapor phase is estimated to be higher than in the liquid phase. It is unlikely that a direct association between methoxide and water is occurring because this reaction is known to be slow ($k^{II} = 1.0 \times 10^{-11}$ cm^3 s^{-1} at 0.5 torr He): Kato, S.; Dang, T. T.; Barlow, S. E.; DePuy, C. H.; Bierbaum, V. M. *Int. J. Mass Spectrom.* **2000**, *196*, 625. For the forward direction in reaction 6 water is present as the neutral reagent ($\sim 5 \times 10^{12}$ molecules cm^{-3}). Again it is unlikely that direct association of hydroxide with water is the major contribution to the hydroxide−water adduct formation, because the rate constant for this process is known to be small ($k^{II} = 1.2 \times 10^{-12}$ cm^3 s^{-1} in 0.5 torr of He), see above: Kato et al.
(59) *N*-Methylpyrazole and *N*-methylimidazole: estimated from DFT (B3LYP/6-311++G(d,p)) calculations (*N*-methylpyrazole $\alpha = 8.88 \times 10^{-24}$ cm^3, $\mu_D = 2.4831$ D; *N*-methylimidazole $\alpha = 8.81 \times 10^{-24}$ cm^3, $\mu_D = 4.2670$ D). H_2O and CH_3OH: *CRC Handbook of Chemistry and Physics*, 75th ed.; Lide, D. R., Ed.; CRC Press: Boca Raton, FL, 1994 (H_2O $\alpha = 1.45 \times 10^{-24}$ cm^3, $\mu_D = 1.854$ D; CH_3OH $\alpha = 3.29 \times 10^{-24}$ cm^3, $\mu_D = 1.70$ D).
(60) Gunion, R. F.; Gilles, M. K.; Polak, M. L.; Lineberger, W. C. *Int. J. Mass Spectrom. Ion Processes* **1992**, *117*, 601.
(61) Koppel, H.; Domcke, W.; Cederbaum, L. S. *Adv. Chem. Phys.* **1984**, *57*, 59.
(62) Trofimov, A. B.; Koppel, H.; Schirmer, J. *J. Chem. Phys.* **1998**, *109*, 1025.
(63) This T_e for the *N*-methyl-5-imidazolyl radical is much smaller than that for the *N*-methyl-5-pyrazolyl radical. This difference reflects the fact that the π orbital in which the unpaired electron resides is localized mostly on the C atoms for the $^2A''$ state of the *N*-methyl-5-imidazolyl radical, while the unpaired electron has significant population on the N atoms as well for the $^2A''$ state of the *N*-methyl-5-pyrazolyl radical. Incidentally, the threefold torsion barrier height for the $^2A''$ state of the *N*-methyl-5-pyrazolyl radical is 431 cm^{-1} according to B3LYP/6-311++G(d,p) calculations. This relatively large barrier height indicates significant hyperconjugation to the methyl group. The corresponding barrier height is 115 cm^{-1} for the *N*-methyl-5-imidazolyl radical where there is little unpaired electron density on the N1 atom.
(64) The largest source of experimental error is due to the measurement of k_r. The presence of a more basic anion would artificially raise the rate constant and proton-transfer branching ratio for the reaction of *N*-methylimidazolide with water, and therefore, the reported proton-transfer rate constant represents an upper bound measurement.
(65) DePuy, C. H.; Kato, S. *Encyclopedia of Mass Spectrometry*; Elsevier: Amsterdam, 2003; Vol. 1, p 670.
(66) *NIST Chemistry WebBook, NIST Standard Reference Database Number 69*; Linstrom, P. J., Mallard, W. G., Eds.; National Institute of Standards and Technology: Gaithersburg, MD, 2005 (http://webbook.nist.gov).
(67) Chase, M. W., Jr.; Davies, C. A.; Downey, J. R., Jr.; Frurip, D. J.; McDonald, R. A.; Syverud, A. N. *J. Phys. Chem. Ref. Data* **1985**, *14*.
(68) Mo, O.; Yanez, M.; Roux, M. V.; Jimenez, P.; Davalos, J. Z.; Ribeiro da Silva, M. A. V.; Ribeiro da Silva, M. d. D. M. C.; Agostinha, M.; Matos, R.; Amaral, L. M. P. F.; Sánchez-Migallón, A.; Cabildo, P.; Claramunt, R.; Elguero, J.; Liebman, J. *J. Phys. Chem. A* **1999**, *103*, 9336.
(69) B3LYP/6-311++G(d,p) calculations predict that $\Delta_{acid}G_{298}$(C5−H, pyrazole) = 376.8 kcal mol^{-1} and D_0(C5−H, pyrazole) = 118.1 kcal mol^{-1}. These values are close to the measured values of *N*-methylpyrazole reported here.
(70) Davico, G. E.; Bierbaum, V. M.; DePuy, C. H.; Ellison, G. B.; Squires, R. R. *J. Am. Chem. Soc.* **1995**, *117*, 2590.
(71) McDonald, R. N.; Bianchina, Jr., E. J.; Tung, C. C. *J. Am. Chem. Soc.* **1991**, *113*, 7115.
(72) The cyclopentadienyl radical is stabilized by delocalization, but the species lacks one electron in the π system for aromaticity under the $4n + 2$ Huckel's rule.
(73) DePuy, C. H.; Kass, S. R.; Bean, G. P. *J. Org. Chem.* **1988**, *53*, 4427.
(74) Villano, S. M.; Gianola, A. J.; Kato, S.; Bierbaum, V. M.; Lineberger, W. C. Manuscript in preparation.